Int J Fract (2006) 139:369–381
DOI 10.1007/s10704-006-0053-z

ORIGINAL ARTICLE

Rupture by damage accumulation in rocks

David Amitrano

Received: 2 November 2005 / Accepted: 27 February 2006

Abstract The deformation of rocks is associated with microcracks nucleation and propagation, i.e. damage. The accumulation of damage and its spatial localization lead to the creation of a macroscale discontinuity, a so-called “fault” in geological terms, and to the failure of the material, i.e., a dramatic decrease of the mechanical properties as strength and modulus. The damage process can be studied both statically by direct observation of thin sections and dynamically by recording acoustic waves emitted by crack propagation (acoustic emission). Here we first review such observations concerning geological objects over scales ranging from the laboratory sample scale (dm) to seismically active faults (km), including cliffs and rock masses (Dm, hm). These observations reveal complex patterns in both space (fractal properties of damage structures as roughness and gouge), time (clustering, particular trends when the failure approaches) and energy domains (power-law distributions of energy release bursts). We use a numerical model based on progressive damage within an elastic interaction framework which allows us to simulate these observations. This study shows that the failure in rocks can be the result of damage accumulation.

Keywords Damage localization · Acoustic emission · Mesoscale modeling

1 Introduction

Deformation of rocks, when loaded at high strain rate and low temperature, involves damage processes such as microfracturing (King and Sammis 1992; Kranz 1983). These low scale defects induce material damage, i.e., reduced elastic and strength properties. As the crack propagation emits acoustic waves, the damage activity can be observed through seismic activity (so called acoustic emission at laboratory sample scale or micro-seismicity at rock massive scale). During the deformation process, the damage localization can lead to the nucleation of a macroscopic discontinuity (faulting) associated with a dramatic stress release which characterizes brittle behavior (Cox and Meredith 1993; Jaeger and Cook 1979; Lockner et al. 1991; Scholz 1990). The change of loading conditions (reduced strain rate, increased temperature or confining pressure) induces a change of the macroscopic behavior, which becomes progressively more ductile (absence of macroscopic stress drop) and on damage repartition, which becomes more diffuse (Jaeger and Cook 1979; Kranz 1983; Menendez et al. 1996). The identification of the parameters

---

D. Amitrano (✉)
LIRIGM, Université J. Fourier, Grenoble, Maison des Geosciences, 1381 rue de la Piscine,
BP 53, 38041, Grenoble Cedex 9, France
e-mail: David.amitrano@ujf-grenoble.fr

controlling both the macroscopic behavior and the spatial damage repartition is an important topic for numerous geomechanics domains (underground excavation, slope instability, dams, earth-crust seismicity), because it determines the ability to predict dramatic ruptures (rockbursts, rock masses collapse, earthquakes, etc.).

The damage localization process in rocks has been often modeled to consider either a discontinuous media containing propagating cracks (Costin 1983; Cowie et al. 1993; Li et al. 2000; Scavia 1995) or a continuous material subject to a bifurcation phenomena (Rice 1975; Rudnicki and Rice 1975). An intermediary approach consists in considering the material to be continuous at mesoscale. The cracking is taken into account through elastic damage (reduction in the apparent elastic modulus). In this way, using local progressive damage and elastic interaction, previous attempts succeeded in modeling either macroscopic plasticity (Zapperi et al. 1997b) or macroscopic brittleness (Tang 1997; Tang and Kaiser 1998). Amitrano et al. (1999), using a local scalar damage formulation associated with a tensorial elastic interaction model, succeeded in switching continuously from macroscopic plasticity, with diffuse damage, to macroscopic brittleness, with localized damage. After these results, the brittle–ductile and localized–diffuse transitions appear to be controlled by a single parameter, the internal friction. These numerical results appear to be in good agreement with laboratory experiments (Amitrano 2003) and earthcrust observations (Gerstenberger et al. 2001; Mori and Abercombie 1997; Schorlemmer and Wiemer 2005; Sue et al. 2002). In this paper we first review experimental observations of failure in rocks, distinguishing static observation of damage structure and dynamic observation of damage dynamics. Then we use a numerical model of progressive damage to show how fracture may result from damage accumulation.

2 Experimental observations of damage in rocks

2.1 Damage structure

During the first steps of the loading of initially intact rocks, microfracturing appears to be homogeneously distributed in the whole material and mainly in mode I. As microfracturing progresses, cooperative interactions of cracks take place and lead to the coalescence of microcracks and the initiation of a macroscopic fracture which is macroscopically in mode II (Amitrano and Schmittbuhl 2002; Costin 1983; Kranz 1983; Reches and Lockner 1994; Schulson et al. 1999). Such a coalescence process has been experimentally observed by acoustic emission source location (Lockner and Byerlee 1991). After failure, or when the discontinuity already exists, deformation is localized along the rupture band. Low-scale observations reveal that the rupture zone or shear band is made of granular material (called gouge or cataclasis in geological terms), filled in between two rupture surfaces. The different aspects of damage—cracks, rupture surface, gouge—that result from the deformation process, can be observed either at the field scale (natural faults) or at the laboratory sample scale (e.g. Keller et al. 1997; Wibberley et al. 2000). Shear deformation occurs both on the rupture surface and within the gouge layer involving friction surface erosion (e.g. Wang and Scholz 1994) and grain fracturing (Biarez and Hicher 1997; Michibayashi 1996). The latter reduces particle size as shear progresses. Thin particles might form subshear bands as observed both at laboratory scale or at field scale (Amitrano and Schmittbuhl 2002; Boullier et al. 2004; Lin 1999; Mair et al. 2000; Menendez et al. 1996; Moore et al. 1989). Each aspect of the damage process during fracturing reveals scaling invariances (King and Sammis 1992; Turcotte 1992). Power-law scaling is found for: crack lengths, crack spatial distributions (Hirata et al. 1987; Velde et al. 1993), rupture surface roughness (Bouchaud 1997; Bouchaud et al. 1990; Brown and Scholz 1985; Schmittbuhl et al. 1993, 1995), and grain-size distribution of the gouge (Amitrano and Schmittbuhl 2002; Boullier et al. 2004; Marone and Scholz 1989; Sammis and Biegel 1989; Weiss and Gay 1998). The self-affine properties of fracture roughness is widely observed in mode I fracture obtained by traction. They have been also observed for fracture resulting from damage localization which is macroscopically mode II (Amitrano and Schmittbuhl 2002). The power-law distribution of grain size has been also observed for gouge sampled within the damaged zone of seismic fault (Boullier et al. 2004).

2.2 Damage dynamics

The mechanical loading of rocks involves local inelastic processes that produce acoustic wave emissions (AE). This provides a tool for following the damage dynamics during the deformation and failure processes. The correlation between AE activity and macroscopic inelastic strain has been established in many experimental (e.g. Lockner and Byerlee 1991; Scholz 1968a) and numerical (e.g. Young et al. 2000) studies. The AE tool has been extensively used at the laboratory rock sample scale (see Lockner 1993 for a review) and at an intermediate scale between the lab scale and the large tectonic earthquakes, for studies of seismicity and rockburst in mines or tunnels (e.g. Nicholson 1992; Obert 1977) and for monitoring slope stability related to either open mine, quarry, landslides, rocky-cliffs or volcano flanks (Amitrano et al. 2005; Hardy and Kimble 1991; e.g. McCauley 1976).

Fracturing dynamics during mechanical loading, observed through AE monitoring, usually displays a power law distribution of acoustic events size (Scholz 1968b).

$$N\,(>A) \sim A^{-b}, \tag{1}$$

where A is the maximum amplitude of AE events, $N(>A)$ is the number of events with maximum amplitude greater than A, b is a constant. In a log-log representation, this distribution appears linear and b is given by the slope of the line.

$$\log N\,(>A) \sim -b \log A. \tag{2}$$

This distribution exhibits remarkable similarity to the Gutenberg–Richter relationship observed for earth-quakes (Gutenberg and Richter 1954).

$$\log N\,(>M) \sim -bM, \tag{3}$$

where $N(>M)$ is the number of earthquakes with a magnitude larger than M. Assuming that the magnitude is proportional to the log of the maximal amplitude of the seismic signal, the b values obtained from the magnitude or the amplitude can be compared (Weiss 1997). Rigorously, the amplitude measured at a given distance from the source should be corrected for the attenuation. Nevertheless, theoretical (Weiss 1997) and experimental studies (Lockner 1993) have shown that attenuation has no significant effect on the b value.

In order to quantitatively estimate the damage localization, many authors use the spatial correlation integral method (Grassberger and Prococcia 1983) for characterizing the distribution of the AE source cloud. The spatial correlation integral is defined as:

$$C\,(r) = \frac{2}{N\,(N-1)} N\,(R > r)\,, \tag{4}$$

where N is the total number of damage events, $N(R > r)$ is the number of pairs of events separated by a distance smaller than r. If this integral exhibits a power law, $C\,(r) \sim r^{D_2}$, the population can be considered as fractal and D_2 is the correlation dimension.

As power laws indicate scale invariance and because of the similarities in the physics of the phenomena (wave propagation induced by fast source motion), AE of rocks observed in the laboratory has been considered as a small scale model for the seismicity in rock masses (rockbursts) or in the Earth's crust (earthquakes) (Mogi 1962; Scholz 1968b). Observations of both earthquakes and AE show variations of the b value in time and space domains which are usually explained using fracture mechanics and/or the self-organized criticality (SOC) concept. Mogi (1962) suggested that the b-value depends on material heterogeneity, a low heterogeneity leading to a low b-value. Scholz (1968b) observed that the b-value decreases before the peak stress is achieved and argued for a negative correlation between b-value and stress. Main et al. (1989) observed the same variation but invoked a negative correlation between the b-value and the stress intensity factor K. Following this idea, the authors proposed different patterns of b-value variation before the macrorupture, driven by fracture mechanics and the type of rupture (brittle–ductile). The relationship between the b-value and the fractal dimension D_2 of AE source locations was also investigated (Lockner and Byerlee 1991; Lockner et al. 1991) and showed a decrease of b-value simultaneous to the strain localization, i.e. to a decrease of the D_2 value which appear to be associated with a ductile macroscopic behavior. Numerical models based on elastic damage (Tang 1997; Tang and Kaiser 1998) succeed in simulating brittle behavior. Discrete element models simulating macroscopic behavior ranging from brittle to ductile and power-law distributions of earthquakes have also been proposed (Li et al. 2000; Place and Mora 2000; Wang et al. 2000). Wang et al. (2000) argue that the *b*-value depends on the cracks density distribution but do not report a relation between the *b*-value and the type of mechanical behavior. Amitrano et al. (1999) and Amitrano (2003) proposed a model which simulates both ductile and brittle behavior and show that the *b*-value depends on the macroscopic behavior. These results suggest that a relationship between the *b*-value and the macroscopic behavior may exist.

Mori and Abercombie (1997) observed a decrease of the *b*-value with increasing depth for earthquakes in California. They suggested that the *b*-decrease was related to a diminution of the heterogeneity as depth increases. Systematic tests of the dependence of the *b* value on depth have been performed by Gerstenberger et al. (2001) which confirm these general results but show some discrepancies depending on the tectonic stress regime. The depth dependence of the *b*-value have also been observed for the western Alps seismicity (Sue et al. 2002) and for earthquakes sequence along the Aswan Lake in Egypt (Mekkawi et al. 2002). Recent results show that the *b*-value depends on the tectonics regime (Schorlemmer and Wiemer 2005) and systematically variate for normal faulting (extension), inverse faulting (compression) and strike-slip (plane shearing). Other authors have used cellular automata (Chen et al. 1991; Olami et al. 1992) or lattice solid models (Zapperi et al. 1997b) to simulate power-law distribution of avalanches.

Acoustic monitoring has been used for studying the damage acceleration before failure. Laboratory scale experiments on heterogeneous material have revealed that the acceleration follows a power law (Guarino et al. 1998; Johansen and Sornette 2000; Nechad et al. 2005). This power law accelerating microdamage before the macroscopic brittle failure has been suggested to be the fingerprint of a critical behavior analog to a thermodynamics phase transition (Buchel and Sethna 1997; Kun and Herrmann 1999; Sornette 2000; Sornette and Andersen 1998; Zapperi et al. 1997a). This kind of acceleration has been recently reported for the seismic events preceding the collapse of a chalk cliff (Amitrano et al. 2005).

Nonetheless, many other experiments do not reproduce the patterns predicted by statistical physics before brittle failure and the applicability of these brittle failure models to the earth crust fracturing is still debated, e.g. the so-called critical point hypothesis for earthquakes (Bufe and Varnes 1993; Jaume and Sykes 1999; Zoller and Hainzl 2002).

3 Numerical modeling

3.1 Progressive damage model

The model we use here (Amitrano 2003; Amitrano et al. 1999) integrates the main features of two previous models which simulate respectively macroscopic ductility (Zapperi et al. 1997b) or brittleness (Tang 1997; Tang and Kaiser 1998). It is based on progressive isotropic elastic damage. The effective elastic modulus, E_{eff}, is expressed as a function of the initial modulus, E_0 and damage, D.

$$E_{\text{eff}} = E_0(1 - D) \tag{5}$$

Such a relation works when the considered volume is large compared with the defect size, such as cracks, and then can be considered as a mesoscale relationship. The damage parameter, D, has been proposed to be related to crack density (see Kemeny and Cook 1986 for a review). The simulated material is discretized using a 2D finite element method with plane strain hypothesis. The loading consists in increasing the vertical displacement of the upper model boundary. When the stress in an element exceeds a given damage threshold, its elastic modulus is multiplied by a factor $(1 - D)$, D being constant. Because of the elastic interaction, the stress redistribution around a damaged element can induce an avalanche of damages that we call an event. The total number of damaged elements during a single loading step is the avalanche size, which is comparable to the acoustic emission event size observed in laboratory experiments.

The Mohr–Coulomb criterion is used as a damage threshold,

$$\tau = \mu\sigma + C, \tag{6}$$

where τ is the shear stress; σ is the normal stress; C is the cohesion; and μ is the internal friction coefficient. This criterion has been chosen because of its simplicity and because it allows us to check the sensitivity of the model to each parameter (C, μ, σ) in an independent manner. In the absence of heterogeneity, the behavior of the model is entirely homogenous, (i.e. no damage localization occurs) and the local behavior is replicated at the macroscopic scale. To obtain macroscopic behaviors differing from those of the elements and damage localization it is necessary to introduce heterogeneity. To simulate material heterogeneity the cohesion of each element, C, is randomly drawn from a uniform distribution.

3.2 Numerical simulation results

The study of the model sensitivity has shown that confining pressure, cohesion and damage parameter D do not change the type of macroscopic behavior, nor the kind of localization mode, but only the macroscopic stress level (Amitrano et al. 1999). On the contrary, the internal friction influences both the macroscopic behavior and the damage localization. Consequently, we present the results obtained with different values of μ and fixed values for the others parameters: $E_{\text{initial}} = 50\,\text{GPa}$, $\nu = 0.25$, C random between 25 and 50 MPa, $D = 0.1$. The simulations are performed with uniaxial stress conditions ($\sigma_2 = \sigma_3 = 0$).

Figure 1 presents the macroscopic behavior simulated for different values of the internal friction μ. σ_1 is the major main stress and ε_1 is the major main strain calculated at the model boundary, i.e., the mean values over the boundary. One may observed that for μ ranging from 0 to 1.5, which corresponds to the variation range observed for rocks, the macroscopic behavior ranges from pure ductility to brittleness, without changing the elementary behavior of the elements. Figure 2 displays the damage map at the end of the simulations for 3 simulations with $\mu = 0$, $\mu = 0.4$ and $\mu = 1$. The color scale bar indicates the damage of each element (i.e. E/E_0). One may observe that damage localization is dramatically enhanced when the μ parameter increases.

In order to estimate quantitatively the grade of damage localization we calculated the correlation integral of the damage at the end of each simulation. The correlation dimension D_2 was calculated by linear regression in the log-log plane. The range used for the linear regression was restricted to the linear part of the curves ($r = 0.01$–0.1). A value of D_2 near 2 indicates that the spatial repartition is homogeneous. A value near 1 indicates that the damage is localized along a line. Figure 3 shows the correlation integrals calculated for all the simulations and the corresponding value of the correlation dimension. These results show that the damage localization progressively increases as the μ parameter is increased. The study of the damage localization during the simulation shows, in the case of brittle behavior (i.e., presence of a stress drop after the stress peak), the band localization occurs during the macrofailure. This is in good agreement with experimental studies using acoustic emission to assess the damage localization process (Lockner and Byerlee 1991). The ductile behavior is associated with a diffuse damage ($D_2 \sim 2$). Note that tuning the μ parameter allows us to simulate all intermediary behaviors from pure ductility to pure brittleness. This progressive change in the macroscopic behavior is associated with a progressive change from diffuse to localized damage.

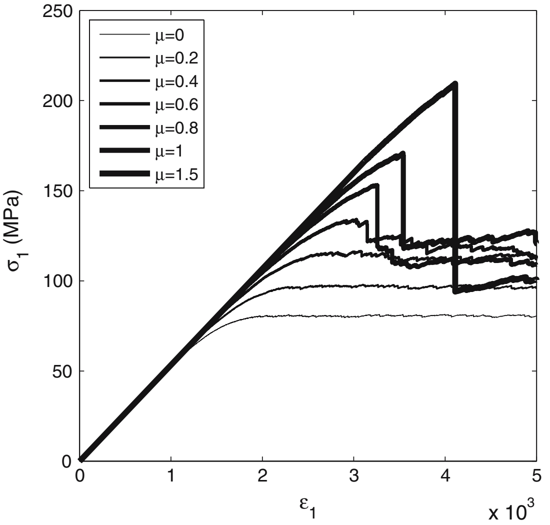

Fig. 1 Macroscopic mechanical behaviors simulated for different μ values. Tuning the μ parameter allows switching continuously for ductile to brittle behaviors

The brittle–ductile behavior appears to be related to the diffuse–localized damage repartition respectively. These results suggest that the

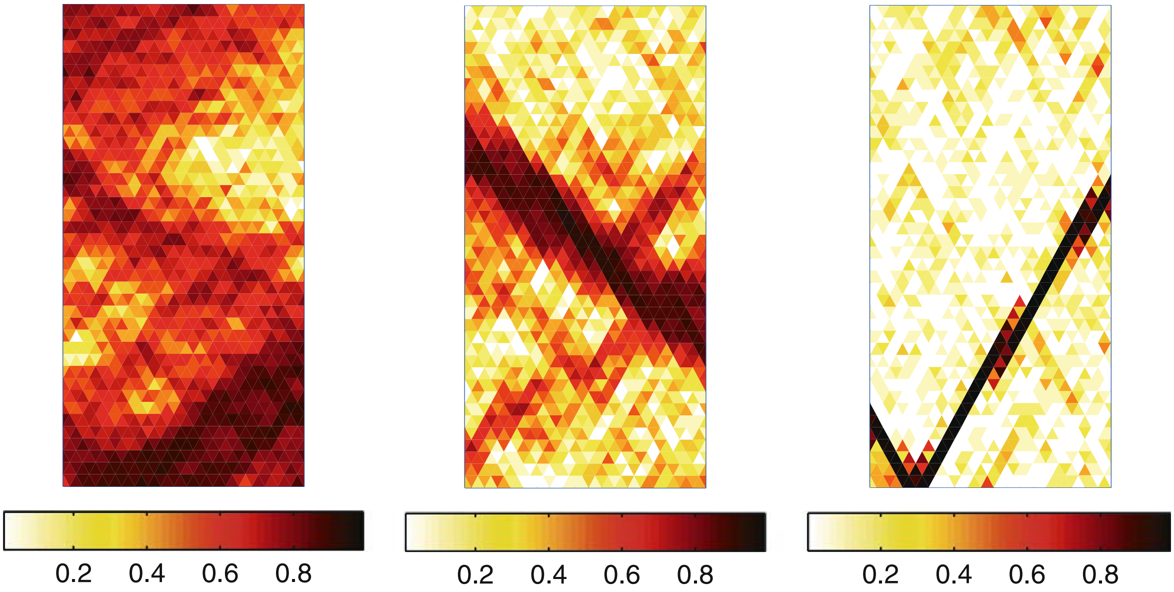

Fig. 2 Damage map for simulation performed with $\mu = 0$ (left), $\mu = 0.4$ (center), $\mu = 1$ (right). The color bar indicates the value of the damage, $D = 1 - E/E_0$. The increase of the μ parameter leads to more localized damage

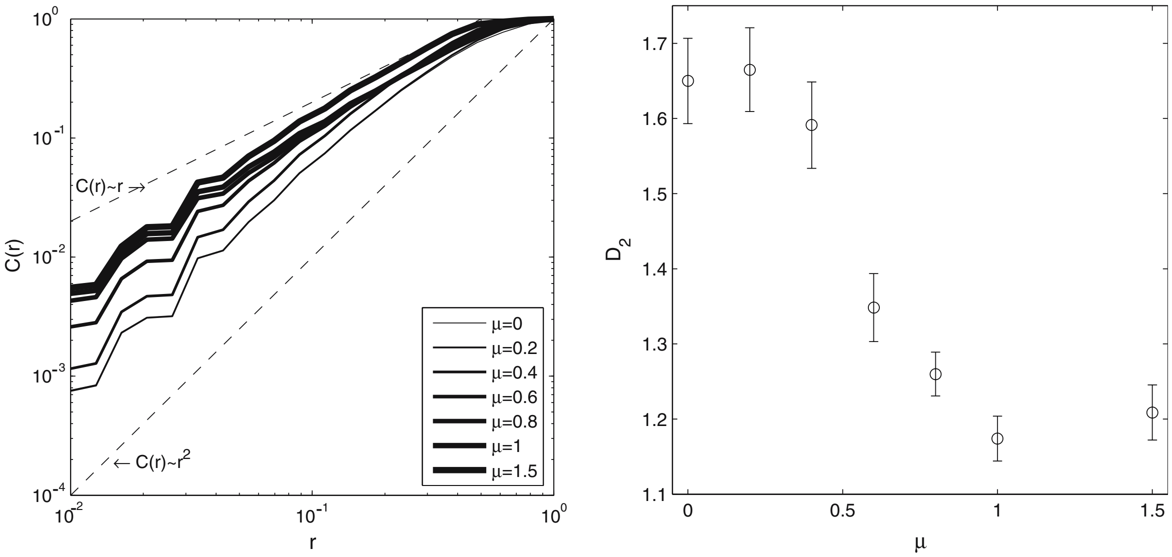

Fig. 3 (**a**) Spatial correlation integral, $C(r)$, of the damage events for various values of μ. (**b**) Correlation dimension, D_2, calculated by least square regression of $C(r)$ in a loglog plot. The regression is restricted to linear part of $C(r)$, i.e. for $r = 0.01$–0.5. Dotted lines indicated particular values of $D_2 = 1$ and $D_2 = 2$

brittle–ductile transition and the associated localized–diffuse transition are controlled by a unique parameter, the internal friction μ. This is in agreement with experimental results for which it has been established that materials with large internal friction tend to fail by localized failure, whereas those with very low internal friction angle fail by a diffuse mode (Jaeger and Cook 1979). Because we use the Mohr–Coulomb criterion, for which the internal friction angle is independent of the confining pressure, the simulated macroscopic behavior is insensitive to the confining pressure. This feature is in disagreement with experimental observations, which demonstrate that the increase of confining pressure induces the brittle–ductile transition. An improvement of the model has been proposed (Amitrano 2003) using a pressure sensitive criterion in order to simulate the pressure-induced brittle–ductile transition. As we focus here on the failure induced by damage accumulation, all the simulations presented here are realized with the simplest first version of the model.

In order to better quantify the spatial structure of the damage, we calculated the directional spatial correlogram (DSC) of the total amount of damage $D = 1 - E/E_0$. For a given direction, $\vec{n}$, the DSC is calculated as the autocorrelation function along this direction, i.e. the correlation between the damage value observed at point x and at point x' separated by a distance λ along direction $\vec{n}$ (at an angle α relatively to the loading direction). The correlation is calculated as the covariance between $D\left(\vec{x}\right)$ and $D\left(\vec{x}+\lambda\vec{n}\right)$ divided by the variance of $D\left(\vec{x}\right)$.

$$\mathrm{DSC}\left(\alpha,\lambda\right) = \frac{\mathrm{var}\left(D\left(\vec{x}\right), D\left(\vec{x}+\lambda\vec{n}\right)\right)}{\mathrm{var}\left(D\left(\vec{x}\right)\right)}. \tag{7}$$

We calculated the DSC as a function of the distance λ for all values of α between 0 and 180°, with a step of 5°. This analysis is able to reveal the spatial correlation of the damage and its anisotropy. The direction of the damage band is characterized by a long range correlation and the perpendicular direction by a correlation length equivalent to the band thickness. Figure 4 shows the DSC for three different simulations performed with $\mu = 0$, $\mu = 0.4$ and $\mu = 1.5$, respectively. DSC was calculated for ten successive steps of the simulation corresponding to an equal number of damage events. The legend indicates the corresponding normalized deformation. The direction α corresponds to the direction of the shear band and $\alpha + \pi/2$ to the shear band normal. One may observe that the correlation length at the beginning of the simulation is near zero for directions α and $\alpha + \pi/2$. This is observed for all the directions, indicating an isotropic damage with no spatial correlation. The damage at a given point is independent of the damage in its neighborhood. As the simulation progress, the correlation length increases in the same manner for all the directions. At a given step the anisotropy appears as the correlation length increases faster in the direction of the future shear band. In the perpendicular direction the correlation becomes negative for a length corresponding to the thickness of the shear band. This progression from isotropic uncorrelated damage to anisotropic correlated damage is observed for all the simulations. An interesting point is that the increase of correlation length appears significantly before the peak stress, including for the brittle behavior. This should be used for the forecasting of macroscopic failure.

The damage event size (i.e. the number of damaged elements in each single avalanche) distribution has been analyzed as a function of the internal friction μ and of the deformation. Figure 5 shows the cumulative distribution function (*cdf*) and the probability density function (*pdf*) of the damage event size for simulations performed with various μ. The *cdf* and *pdf* show power law trends in the range 1–100. For larger size events, *cdf* displays a cut-off (lack of large events compared to the power-law trend) for low values of μ. As μ increases this cut-off progressively vanishes. For larger values of μ the cut-off is replaced by an excess of large events compared to the power-law trend. The larger event corresponds in this last case to the macro failure event.

Figure 6 shows the evolution of *cdf* during the deformation for two simulations with $\mu = 0$ and $\mu = 1.5$, respectively. For both simulations the *cdf* displays a power law trend, for low size events with a decrease of the exponent. For $\mu = 0$, this decrease is associated with a cut-off for large sizes. For $\mu = 1.5$ the decrease is of lesser amplitude and no cut-off appears. On the contrary, an excess of large events appears in the period including the macro failure which is out of trend compared with the power law.

4 Summary and discussion

In the first part of the paper we have reviewed works related to the observation of rupture in rocks which reveal complex patterns including fractal properties of damage structure, as self-affinity of fracture surfaces and power-law distribution of grain size in highly damaged zones. The damage dynamics, as observed by acoustic emission, displays power-law distributions with exponent value

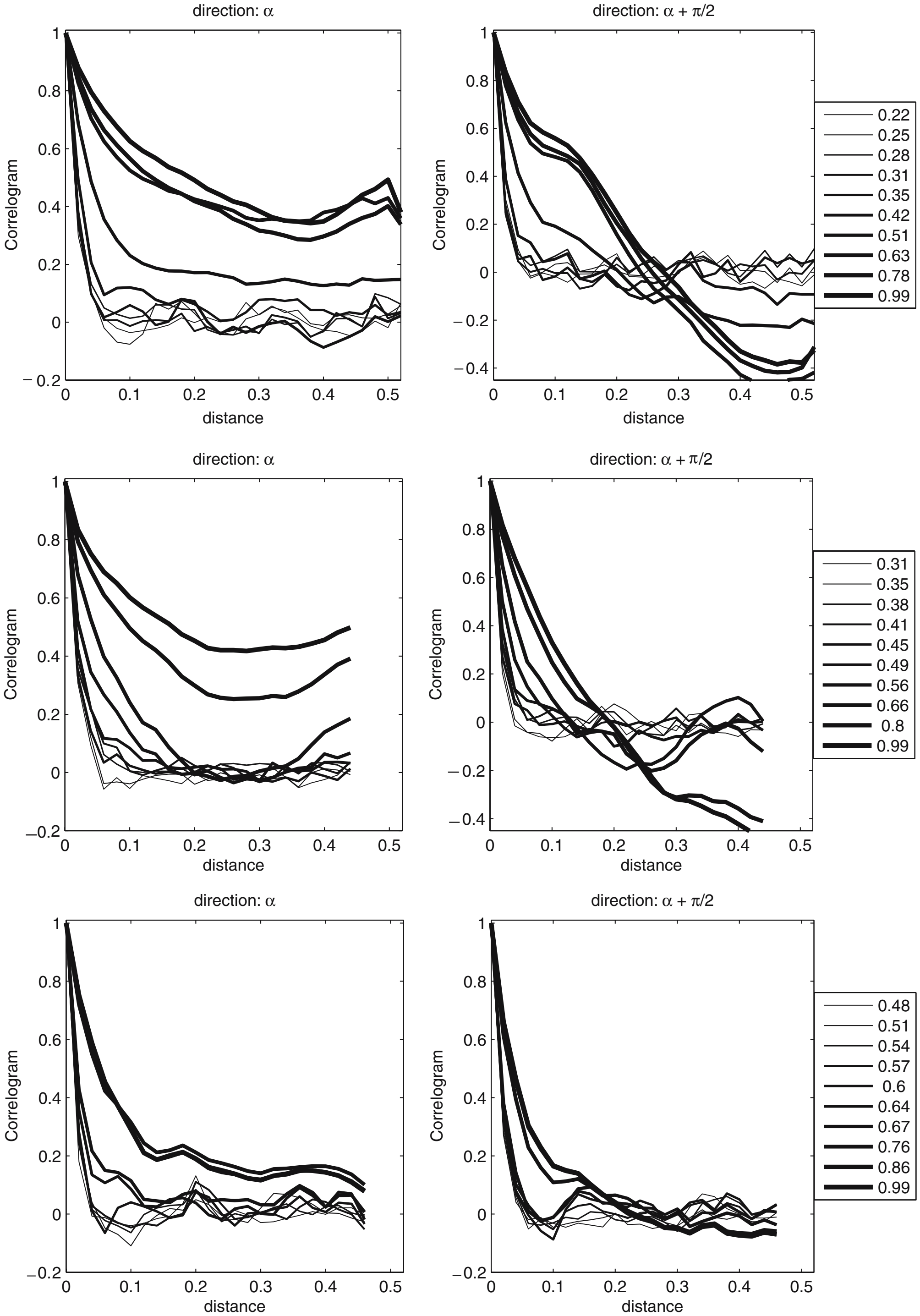

Fig. 4 Damage spatial correlogram (DSC) calculated for three different simulations ($\mu = 0$, $\mu = 0.4$, $\mu = 1.5$ from top to bottom). DSC is calculated for successive steps. DSC is calculated for ten successive steps of the simulation corresponding to an equal number of damage events. The legend indicates the corresponding normalized deformation. The direction α corresponds to the direction of the shear band and $\alpha + \pi/2$ to the perpendicular

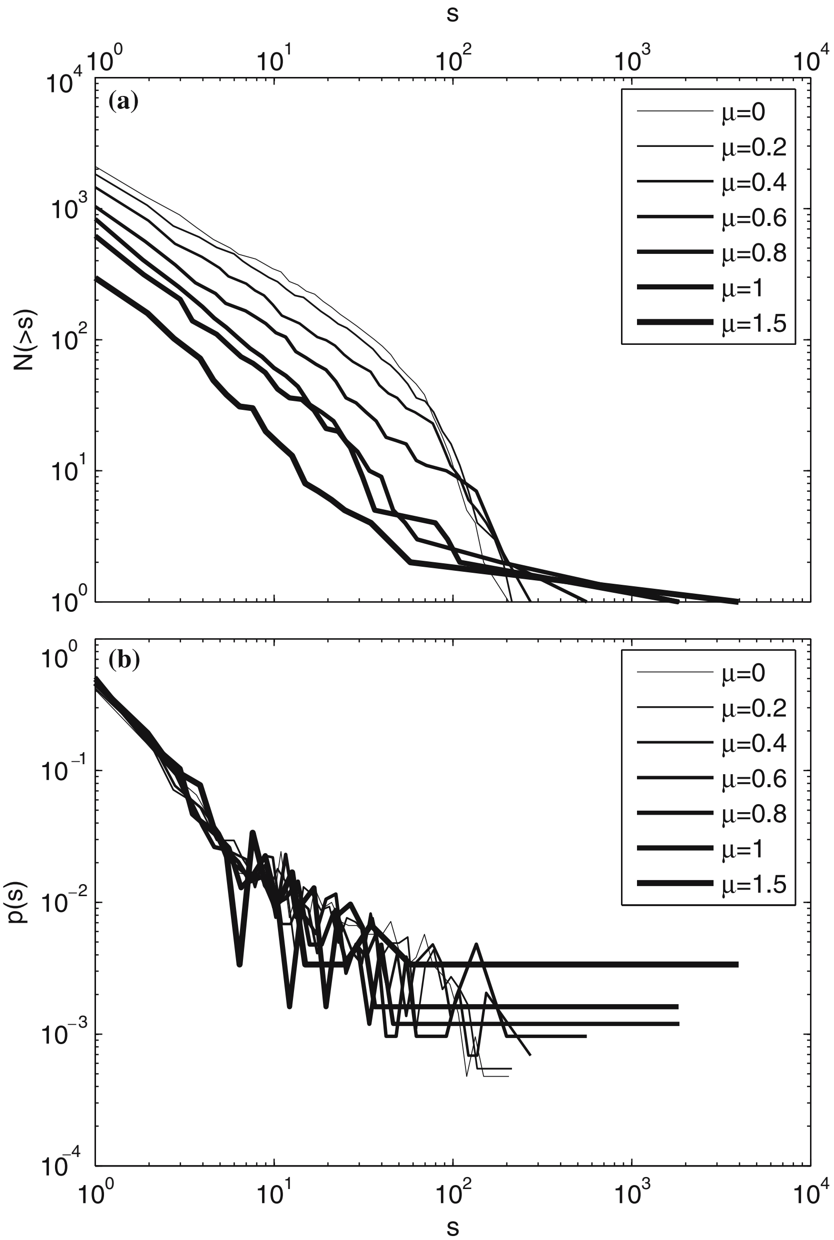

Fig. 5 (**a**) Cumulative distribution function (*cdf*), and (**b**) probability density function (*pdf*) of the damage event size for simulations performed with various μ

depending on the pressure and on the proximity of the failure. The final failure of the material appears to be the result of damage localization/accumulation. For investigating this process we used a simple progressive damage model able to reproduce the major part of these observations.

The proposed model is based on an elementary progressive damage within an elastic heterogeneous model. Each element has isotropic properties associated with a simple behavior, i.e., decrease of the elastic modulus by discrete damage events. At the macroscopic scale, the model reproduce different aspects of a complex behavior: the mechanical behavior is non-linear and ranges from ductile to brittle, the final damage state has a fractal structure, the size-frequency of damage

Fig. 6 Cumulative distribution function for $\mu = 0$ and $\mu = 1.5$. The *cdf* has been calculated for five successive steps of equal number of events. The legend indicates the corresponding range of normalized deformation

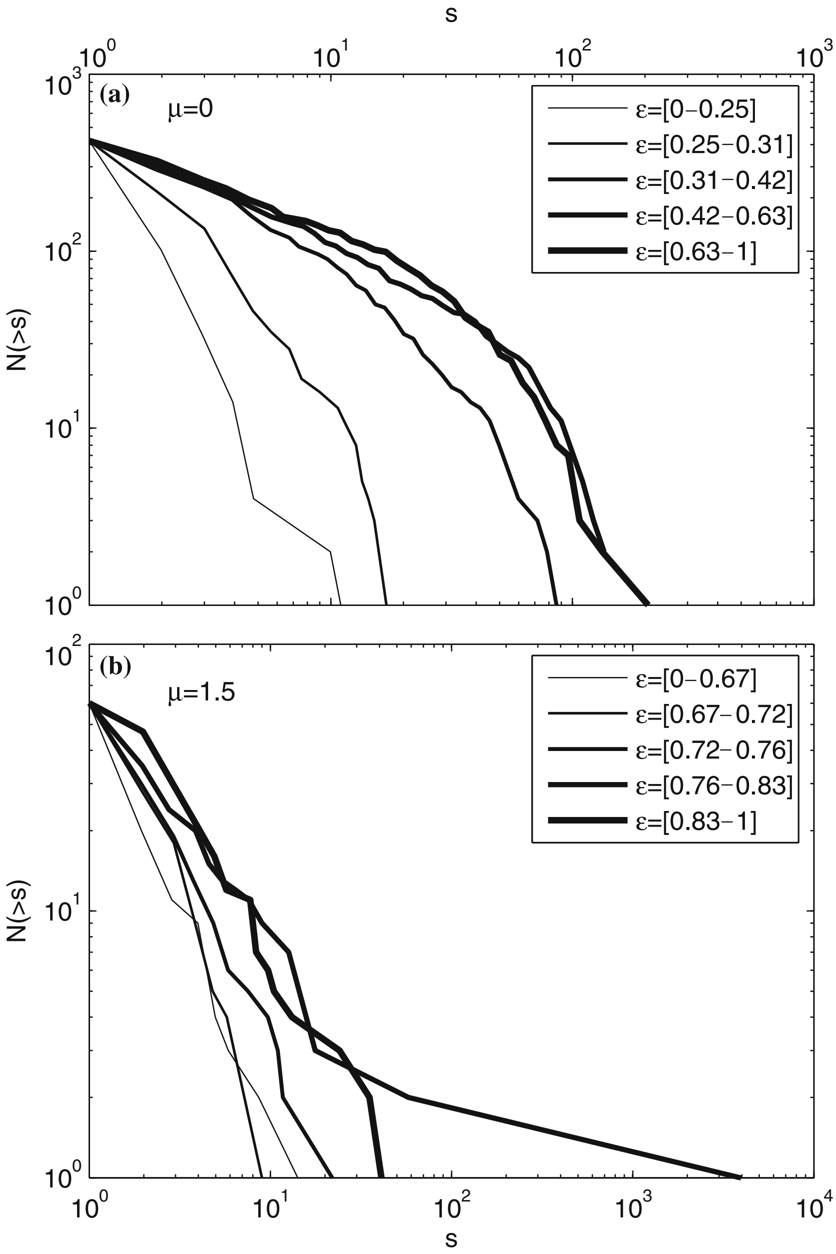

events follows a power-law. As these properties are not incorporated at the elementary scale, they are emerging properties of the system due to the interaction between elements. According to that, the simulated deformation process can be considered as a complex system. The emergence of scale free distributions for both size and space distributions is a supplementary aspect of this complexity. We have shown that changing the internal friction μ modifies all the macroscopic properties. In particular, we have observed that the damage localization is dramatically enhanced when the μ parameter increases. The study of the stress field around a single defect (Amitrano et al. 1999), has shown that this parameter strongly influences the interaction geometry between elements. The higher the μ

parameter is, the more anisotropic the interaction is. This low scale anisotropic interaction controls the mode of damage localization we can observe at the macroscopic scale. In the case of a highly localized damage (i.e. for $\mu > 1$), the localization occurs in an instable mode associated with a dramatic stress drop, we considered as the fingerprint of a macroscopically brittle behavior. The μ parameter influences also the event size distribution as a result of the local interaction between elements (more or less anisotropic). Hence the small scale anisotropy influences the damage localization, the avalanches dynamics and the macroscopic behavior. Despite the limited scale dynamics of the model, we observed the scaling relationship for damage structure, over 1.5 order of magnitude, characterized by a power-law trend of the spatial correlation integral. The event size distribution is a power-law which evolves during the simulation showing a decrease of the exponent, i.e. an increase of the event mean size, in agreement with laboratory observation. In the brittle case, the failure corresponds to the larger event in size, which is out of range compared with the power-law trend. The study of spatial correlation of the damage during the simulation has shown an increase of the correlation length more pronounced in the direction of the localization band. This increase of length is associated with the event size increase. The failure occurs when correlation length becomes large enough for leading to a macrofailure event, i.e. the size of the model.

These numerical results show that damage accumulation leading to the failure is strongly influenced by the local interaction geometry which, depending on the anisotropy, can lead either to a macroscopically ductile behavior with progressive localization, i.e., without stress drop, or to a macroscopically brittle behavior associated to a sudden localization event. All these results are obtained without changing the basic elementary behavior but only the interaction. This mesoscale approach could be an alternative to the microscopic approach, dedicated to the study of fracture propagation and to the macroscopic approach based on constitutive laws. It provides observables which are emerging properties from elementary interaction and, in this regard, consider the rupture process as a complex phenomenon.

5 Conclusions

We have shown that the deformation and rupture process in rocks reveals many complex behaviors as fractal structure of damage, power-law distribution of damage events, damage localization associated to brittleness/ductility. Using a simple model based on elastic interaction and progressive damage we succeed in reproducing the major part of this complexity. The study of damage spatial correlation revealed that the process of damage localization is related to the passage from isotropic uncorrelated damage to anisotropic correlated damage. The differences in the localization mode (more or less diffuse and progressive) are related to the type of local interaction between elements which can be tuned, in the model we used, by changing the internal friction. Such a mesoscopic approach could be an alternative to the microscopic one based on fracture mechanics concept or to the macroscopic one based on constitutive laws.

References

Amitrano D (2003) Brittle-ductile transition and associated seismicity: experimental and numerical studies and relationship with the b-value. J Geophys Res 108(B1):2044, doi:10.1029/2001JB000680

Amitrano D, Schmittbuhl J (2002) Fracture roughness and gouge distribution of a granite shear band. J Geophys Res 107(B12, 2375):16, doi:10.1029/2002JB001761

Amitrano D, Grasso J-R, Hantz D (1999) From diffuse to localized damage through elastic interaction. Geophys Res Lett 26(14):2109–2112

Amitrano D, Grasso JR, Senfaute G (2005) Seismic precursory patterns before a cliff collapse and critical-point phenomena. Geophys Res Lett 32(8):L08314, doi:10.1029/2004GL022270

Biarez J, Hicher P-Y (1997) Influence de la granulometrie et de son evolution par rupture de grains sur le comportement mécanique des materiaux granulaires. Rev Francaise de genie Civil 1(4):607–631

Bouchaud E (1997) Scaling properties of cracks. J Phys Condens Matter 9:4319–4344

Bouchaud E, Lapasset G, Plane's J (1990) Fractal dimension of fractured surfaces: a universal value? Europhys Lett 13:73–79

Boullier AM, Fujimoto K, Ito H, Ohtani T, Keulen N, Fabbri O, Amitrano D, Dubois M, Pezard P (2004) Structural evolution of the Nojima fault (Awaji Island, Japan) revisited from the GSJ drillhole at Hirabayashi. Earth, Planets Space, 56:1233–1240

Brown SR, Scholz CH (1985) Broad bandwith study of the topography of natural rock surface. J Geophys Res 90(B14):12575–12582

Buchel A, Sethna JP (1997) Statistical mechanics of cracks: fluctuations, breakdown, and asymptotics of elastic theory. Phys Rev E 55(6):7669–7690

Bufe CG, Varnes DJ (1993) Predictive modeling of the seismic cycle and of the greater San francisco Bay region. J Geophys Res 98:9871–9883

Chen K, Bak P, Obukhov SP (1991) Self-organized criticality in a crack-propagation model of earthquakes. Phys Rev A 43(2):625–630

Costin LS (1983) A microcrack model for the deformation and failure of brittle rock. J Geophys Res 88(B11):9485–9492

Cowie P, Vanneste C, Sornette D (1993) Statistical physics model for the spatiotemporal evolution of faults. J Geophys Res 98(B12):21809–21821

Cox SJD, Meredith PG (1993) Microcrack formation and material softening in rock measured by monitoring acoustic emission. Int J Rock Mech Min Sci Geomech Abstr 30(1):11–24

Gerstenberger M, Wiemer S, Giardini D (2001) A systematic test of the hypothesis that *b* varies with depth in California. Geophys Res Lett 28(1):57–60

Grassberger P, Prococcia I (1983) Measuring the strangeness of stange attractors. Physica 9:189–208

Guarino A, Garcimartin A, Ciliberto S (1998) An experimental test of the critical behaviour of fracture precursors. Eur Phys J B 6(1):13–24

Gutenberg B, Richter CF (1954) Seismicity of the earth and associated phenomena. Princeton University Press, Princeton.

Hardy HR, Kimble EJ (1991) Application of high-frequency AE/MS techniques to rock slope monitoring. In: Hardy (ed) Vth Conf. AE/MS Geol. Str. and Mat. Trans Tech Publication, Germany, The Pennsylvania State University, pp 457–477

Hirata T, Satoh T, Ito K (1987) Fractal structure of spacial distribution of microfracturing in rock. Geophys J R astr Soc 90:369–374

Jaeger JC, Cook NGW (1979) Fundamentals of rock mechanics. Chapman and Hall, London, 593 pp

Jaume SC, Sykes LR (1999) Evolving towards a critical point: a review of accelerating seismic moment/energy release prior to large and great earthquakes. Pageoph 155:279–305

Johansen A, Sornette D (2000) Critical ruptures. Eur Phys J B 18:163–181

Keller JVA, Hall SH, McClay KR (1997) Shear fracture pattern and microstructural evolution in transpressional fault zones from field and laboratory studies. J Struct Geol 19(9):1173–1187

Kemeny J, Cook NGW (1986) Effective moduli, non-linear deformation and strength of a cracked elastic solid. Int J Rock Mech Min Sci Geomech Abstr 23(2):107–118

King GCP, Sammis CG (1992) The mechanisms of finite brittle strain. Pageoph 138(4):611–640

Kranz RL (1983) Microcracks in rocks: a review. Tectonophysics 100:449–480

Kun F, Herrmann HJ (1999) Transition from damage to fragmentation in collision of solids. Phys Rev E 59:2623–2632

Li HL, Bai YL, Xia MF, Ke MF, Yin XC (2000) Damage localisation as a possible precursor of earthquake rupture. Pageoph 157:1929–1943

Lin A (1999) S-C cataclasite in granitic rock. Tectonophysics 304:257–273

Lockner DA (1993) The role of acoustic emission in the study of rock fracture. Int J Rock Mech Min Sci Geomech Abstr 30(7):883–899

Lockner DA, Byerlee JD (1991) Precursory AE patterns leading to rock fracture. In: Hardy (ed) Vth Conf. AE/MS Geol. Str. and Mat. Trans Tech Publication, Germany, The Pennsylvania State University, pp 45–58

Lockner DA, Byerlee JD, Kuskenko V, Ponomarev A, Sidorin A (1991) Quasi-static fault growth and shear fracture energy in granite. Nature 350:39–42

Main IG, Meredith PG, Jones C (1989) A reinterpretation of the precursory seismic b-value anomaly from fracture mechanics. Geophys J 96:131–138

Mair K, Main I, Elphick S (2000) Sequential growth of deformation bands in the laboratory. J Struct Geol 22:25–42

Marone C, Scholz CH (1989) Particle-size distributions and microstructures within simulated fault gouge. J Struct Geol 11(7):799–814

McCauley ML (1976) Microsonic detection of landslides, 54th T.R.B annual meeting. Transportation Research Record 581, Washington DC, pp 25–30

Mekkawi M, Hassoup A, Grasso JR, Schnegg PA (2002) Fractal and spectral analysis of the earthquake sequences along the Aswan Lake, Egypt. 26th General Assembly of the European Geophysical Society, Nice, abstract n°EGS02-A-00027

Menendez B, Zhu W, Wong T-F (1996) Micromechanics of brittle faulting and cataclastic flow in Berea Sandstone. J Struct Geol 18(1):1–16

Michibayashi K (1996) The role of intragranular fracturing on grain size reduction in feldspar during mylonitization. J Struct Geol 18(1):17–25

Mogi K (1962) Magnitude frequency relations for elastic shocks accompanying fractures of various materials and some related problems in earthquakes. Bull Earthquake Res Inst Univ Tokyo 40:831–853

Moore DE, Summers R, Byerlee JD (1989) Sliding behavior and deformation textures of heated illite gouge. J Struct Geol 11(3):329–342

Mori J, Abercombie RE (1997) Depth dependence of earthquake frequency-magnitude distributions in California: implication for rupture initiation. J Geophys Res 102(B7):15081–15090

Nechad H, Helmstetter A, Guerjouma RE, Sornette D (2005) Andrade and critical time-to-failure laws in fiber-matrix composites: experiments and model. J Mech Phys Solids 53(5):1099–1127

Nicholson C (1992) Recent developments in rockburst and mine seismicity research. In: Wawersik TA (ed) Rock mechanics. Balkema, Rotterdam, pp 1079–1086

Obert L (1977) The microseismic method: discovery and early history. 1st Conf. AE/MS Geol. Str. and Mat. Trans Tech Publications, pp 11–12

Olami Z, Feder HJS, Christensen K (1992) Self-organised criticality in a continuous, nonconservative cellular automaton modeling earthquake. Phys Rev Lett 68(8):1244–1247

Place D, Mora P (2000) Numerical simulation of Localisation phenomena in a fault zone. Pageoph 157:1821–1845

Reches Z, Lockner DA (1994) Nucleation and growth of faults in brittle rocks. J Geophys Res 99(B9):18159–18173

Rice J (1975) On the stability of dilatant hardening for saturated rock masses. J Geophys Res 80(11):1531–1536

Rudnicki JW, Rice J (1975) Conditions for the localization of deformation in pressure- sensitive dilatant materials. J Mech Phys Solids 23:371–394

Sammis CG, Biegel RL (1989) Fractals, fault-gouge, and friction. Pageoph 131(1/2):255–271

Scavia C (1995) A method for the study of crack propagation in rock structures. Geotechnique 45(3):447–463

Schmittbuhl J, Gentier S, Roux S (1993) Field measurements of the roughness of fault surfaces. Geophys Res Lett 20(8):639–641

Schmittbuhl J, Schmitt F, Scholz C (1995) Scaling invariance of crack surface. J Geophys Res 100(B4):5953–5973

Scholz CH (1968a) Microfracturing and the inelastic deformation of rocks in compression. J Geophys Res 73:1417–1432

Scholz CH (1968b) The frequency-magnitude relation of microfracturing in rock and its relation to earthquakes. Bull Seismol Soc Am 58(1):399–415

Scholz HC (1990) The mechanics of earthquakes and faulting. Cambridge University Press.

Schorlemmer D, Wiemer S (2005) Microseismicity data forecast rupture area. Nature 434:1086, doi: 10.1038/4341086a

Schulson EM, Illiescu D, Renshaw CE (1999) On the initiation of shear faults during brittle compressive failure: A new mechanism. J Geophys Res 104(B1):695–705

Sornette D (2000) Critical phenomena in natural sciences, chaos, fractals, self organization and disorder: concepts and tools. Berlin, New-York, 432 pp

Sornette D, Andersen JV (1998) Scaling with respect to disorder in time-to-failure. Eur Phys J B 1:353–357

Sue C, Grasso JR, Lahaie F, Amitrano D (2002) Mechanical behavior of western alpine structures inferred from statistical analysis of seismicity. Geophys Res Lett 29(8):65–1–65–4, doi:10.1029/2001GL014050)

Tang CA (1997) Numerical simulation of progressive rock failure and associated seismicity. Int J Rock Mech Min Sci Geomech Abstr 34(2):249–261

Tang CA, Kaiser PK (1998) Numerical simulation of cumulative damage and seismic energy release during brittle rock failure – Part I: Fundamentals. Int J Rock Mech Min Sci Geomech Abstr 35(2):113–121

Turcotte (1992) Fractals and chaos in geology and geophysics. Cambridge University Press, 220 pp

Velde B, Moore D, Badri A, Ledesert B (1993) Fractal analysis of fractures during brittle to ductile changes. J Geophys Res 98(B7):11935–11940

Wang W, Scholz CH (1994) Wear processes during frictional sliding of rocks: a theoretical and experimental study. J Geophys Res 99(B4):6789–6799

Wang YC, Yin XC, Ke MF, Xia MF, Peng KY (2000) Numerical simulation of rock failure and earthquake process on mesoscopic scale. Pageoph 157:1905–1928

Weiss J (1997) The role of attenuation on acoustic emission amplitude distributions and b-values. Bull Seismol Soc Am 87(5):1362–1367

Weiss J, Gay M (1998) Fracturing of ice under compression creep as revealed by a multifractal analysis. J Geophys Res 103(B10):24005–24016

Wibberley CAJ, Petit J-P, Rives T (2000) Micromechanics of shear rupture and the control of normal stress. J Struct Geol 22:411–427

Young RP, Hazzard JF, Pettitt WS (2000) Seismic and micromechanical studies of rock fracture. Geophys Res Lett 27(12):1767–1770

Zapperi S, Ray P, Stanley HE, Vespignani A (1997a) First-order transition in the breakdown of disordered media. Phys Rev Lett 78:1408–1411

Zapperi S, Vespignani A, Stanley E (1997b) Plasticity and avalanche behavior in microfracturing phenomena. Nature 388(14 august 1997):658–660

Zoller G, Hainzl S (2002) A systematic spatiotemporal test of the critical point hypothesis for large earthquakes. Geophys Res Lett 29(11):1558, 10.1029/2002GL014856